

# Grain Boundary Induced Magneto-Far Infrared Resonances in Superconducting $\text{YBa}_2\text{Cu}_3\text{O}_{7-\delta}$ Thin Films

H.-T. S. Lihn, E.-J. Choi, S. Kaplan, H. D. Drew

*Center for Superconductivity Research, Physics Department, University of  
Maryland, College Park, MD 20742*

*and*

*Laboratory for Physical Sciences, College Park, MD 20740*

Q. Li and D. B. Fenner

*Advanced Fuel Research, East Hartford, Connecticut 06138*

(April 1, 2018)

## Abstract

Spectral features induced by  $45^\circ$  in-plane misoriented grains have been observed in the far infrared magneto-transmission of  $\text{YBa}_2\text{Cu}_3\text{O}_{7-\delta}$  thin films. Two strong dispersive features are found at 80 and 160  $\text{cm}^{-1}$  and a weaker one at 116  $\text{cm}^{-1}$ . The data can be well represented by Lorentzian oscillator contributions to the conductivity. Several possible interpretations are discussed. We conclude that the resonances are due to vortex core excitations.

PACS numbers: 74.25.Nf, 74.60.Ge, 61.72.M, 74.72.Bk.

Typeset using REVTeX

The electronic properties of superconductors are strongly affected by the application of magnetic fields. The effects range from the quantum interference in Josephson junctions to dissipation in current carrying wires. These effects present interesting physical questions as well as important challenges for superconductivity applications. For example the Hall coefficient is generally observed to reverse sign in the superconducting state, and in some cases even reverse back before vanishing at temperatures well below  $T_c$  due to pinning of the vortex lattice [1]. This behavior is known to be a consequence of the complex dynamics of vortex motion in the presence of viscous and pinning forces but is not yet well understood [2,3]. Indeed controversies about such fundamental issues as the vortex effective mass [4] and the magnetic force on the moving vortex [2] remain unresolved after decades of study of vortex dynamics. The early theories were essentially phenomenological but recently efforts have been devoted to the development of theories of vortex dynamics based on microscopic physics [5,6]. The phenomenological models have been extensively employed in describing the microwave losses [7]. Since many of the characteristic frequencies of the vortex system lie above microwave frequencies, recent high frequency measurements on high  $T_c$  superconductors have greatly expanded the available phenomenology of this subject. Pulsed terahertz experiments on  $\text{YBa}_2\text{Cu}_3\text{O}_{7-\delta}$  (YBCO) have shown a strongly temperature dependent ac Hall signal that has been interpreted in terms of the response of thermally excited quasiparticles near the nodes of a d-wave gap in YBCO [8]. At higher frequencies (but below the IR gap) two chiral resonances have been reported above which the system exhibits free hole-like optical activity [9,10]. The chiral resonances have been identified as the pinning resonance and the vortex core resonance within a clean limit theory of vortex dynamics developed by T. C. Hsu [5]. In this picture the bare resonances are hybridized with the underlying cyclotron resonance of the holes and they are observable only because of the presence of the vortex pinning.

In this paper we present an investigation of the far infrared (FIR) magneto-optics of YBCO films containing large-angle misoriented in-plane grains. The grain boundaries provide a reduced symmetry for pinned vortices which can be expected to alter the selection

rules for optical transitions in the vortex core. However, grain boundaries are also known to modify the electronic properties of superconductors even in zero magnetic field. The microstructure of various types of grain boundaries in YBCO films have been studied by electron energy loss spectroscopy (EELS) together with transmission electron microscopy (TEM) [11–13]. Hole depletion is found that extends as far as  $60\text{\AA}$  from asymmetric grain boundaries, whereas for symmetric grain boundaries the hole density remains essentially constant. They can act as weak link Josephson junctions and enhance the microwave losses [14,15]. In long junctions standing wave Josephson modes can be excited leading to Fiske steps in the I-V characteristics [16]. Also, spectral features in the tunneling conductance have been reported on a single grain boundary [17]. Both of these effects are strongly perturbed by the application of a magnetic fields [16,17].

We report far infrared magneto-optical transmission measurements on YBCO films with varying densities of  $45^\circ$  oriented grains [18]. Induced resonant spectral features are observed superposed on magneto-optical features observed on samples with low densities of  $45^\circ$  grains reported earlier and discussed in terms of vortex dynamics. [10,19] The magnetic field dependence and temperature dependence of the spectra are studied and the spectral line shapes of the induced features are analyzed using a Lorentzian oscillator curve fitting. The possible origin of these resonances is discussed.

The samples are YBCO thin films grown by Pulsed Laser Deposition (PLD) on silicon substrates with yttria stabilized zirconia (YSZ) buffer layers and cap layers. The film thickness is typically  $400\text{\AA}$  and typical critical temperatures are  $T_c = 89\pm 1^\circ\text{K}$  measured by ac susceptibility. Patterned line critical current densities are  $J_c \approx 2 * 10^6\text{A/cm}^2$  at  $77^\circ\text{K}$  [20]. X-ray rocking curve measurements show that c-axis alignment is typically within  $0.7^\circ$ , which is comparable with samples grown on  $\text{LaAlO}_3$  substrates. The morphology of the films is studied by X-ray diffraction. X-ray  $\phi$  scans performed on the (205) plane show that the samples fall into two classes: (1) Films having appreciable densities of low angle grains but no measurable high angle grains. (2) Films showing a high concentration of high angle (mainly  $45^\circ$ ) in-plane grains, but little or no low angle grains. In the samples from Class

(2), the  $45^\circ$  signal is as large as 4% relative to the signal from the grains aligned with the substrate. Although these samples were not especially grown for misoriented grains it is known that the density of  $45^\circ$  grains increases with the growth temperature.

The transmission of the films is measured with a fast scan FTIR spectrometer using a 2.2°K bolometer detector. External magnetic fields up to 12T are applied perpendicular to the a-b plane of the YBCO thin films and the sample temperature is varied from 2.2°K to above  $T_c$ . The incident FIR radiation is elliptically polarized by a polarizer comprised of a metal grid linear polarizer and a 0.9mm thick x-cut quartz waveplate placed in front of the samples. The peak efficiency of the polarizer for circular polarization is at  $65\text{ cm}^{-1}$  and  $160\text{ cm}^{-1}$ . The transmission coefficient is related to the conductivity by  $T^\pm(H) = 4n / |(Z_0 d \sigma^\pm(H) + n + 1)|^2$  where  $\sigma^{+(-)}(H)$  is the circularly polarized conductivity in hole cyclotron resonance (hCR) active (inactive, or eCR) mode,  $d$  is the thickness of the YBCO film,  $Z_0$  is the free space impedance and  $n$  is the refractive index of the silicon substrate. The elliptically polarized transmission data was transformed to the circular polarized response,  $T^\pm(H)$ , using a calibration of the polarizer efficiency based on the cyclotron resonance of a two dimensional electron gas in a high mobility GaAs quantum well [9,21]. Since the efficiency of the polarizer is a slowly varying function over a wide frequency range, the unfolding introduces little error to the spectral features except when the polarizer is close to the half waveplate condition at about  $130\text{ cm}^{-1}$ . A more detailed description of the experiment and data manipulation is given elsewhere [9,10,19].

The transmission ratio  $T^\pm(H)/T(0)$  of samples from Class (1) and (2) at 12T and 2.2°K are shown in Figure 1. The lower (upper) curves  $T^{+(-)}(H)/T(0)$  are in hCR (eCR) mode. The measurement errors become large below  $40\text{ cm}^{-1}$  due to the low transmitted intensity and in the region between  $125\sim 140\text{ cm}^{-1}$  due to a quartz phonon and the half waveplate condition of the polarizer. The transmission curves of Class (1) samples are generally smooth except a for a small broad peak feature at  $65\text{ cm}^{-1}$  in the eCR mode and a sharp rise below  $50\text{ cm}^{-1}$  in the hCR mode. In addition, the transmission ratio approaches unity approximately as  $\omega^{-1}$  at high frequencies in both modes. These features have been observed in many

high quality YBCO samples and they are qualitatively independent of the detailed sample quality, growth technique and choice of substrates. As can be seen from the figure these spectral features are also present in Class (2) samples. We have attributed these canonical features to the electrodynamic response of pinned vortices [10,19].

The conventional theories of vortex dynamics do not properly describe the far infrared magneto-optical response of class (1) samples [7]. In these theories the conductivity has only one resonance and it is at zero frequency with a width that depends on vortex viscosity  $\eta$ . In particular, the optical activity  $T^+(H)/T^-(H)$  observed in the FIR experiments is absent. A recently developed clean limit theory of vortex dynamics by T. C. Hsu does successfully describe the FIR experiments on class (1) samples [5,10]. In Hsu's picture, the small feature in  $T^+(H)/T(0)$  at  $65 \text{ cm}^{-1}$  is due to the hybridized vortex core resonance and the sharp rise below  $50 \text{ cm}^{-1}$  in  $T^-(H)/T(0)$  is the high frequency part of the hybridized pinning resonance. The experiments do not measure down to sufficiently low frequencies to fully resolve this pinning resonance [22]. The high frequency optical activity is a consequence of these two chiral resonances.

Comparing the spectra of the two classes of samples, several differences are observed and these differences are the subject of this paper. There are several induced dispersive features, centered around  $80$ ,  $116$ , and  $160 \text{ cm}^{-1}$ , superimposed on spectra of the class (1) form. This distribution suggests a periodicity of  $\sim 40 \text{ cm}^{-1}$ . In addition, the feature at  $80 \text{ cm}^{-1}$ , which occurs in the hCR mode only, is rather wide extending about  $40 \text{ cm}^{-1}$ , and in fact it appears that it may be a doublet consisting of features at  $72 \text{ cm}^{-1}$  and  $90 \text{ cm}^{-1}$ . The features at  $116 \text{ cm}^{-1}$  and  $160 \text{ cm}^{-1}$  occur with nearly equal weight in both modes. The  $116 \text{ cm}^{-1}$  feature is quite narrow, about  $10 \text{ cm}^{-1}$  wide compared with a width of about  $20 \text{ cm}^{-1}$  for the  $160 \text{ cm}^{-1}$  feature.

The magnetic field dependence of  $T^\pm(H)/T(0)$  of a Class (2) sample is shown in Figure 2. The amplitudes of the grain boundary induced features in Figure 1 are seen to grow approximately linearly with magnetic field and there is no measurable shift in their frequency positions. This observation suggests an interpretation in terms of vortex dynamics since

the vortex density is proportional to the magnetic field and since the energy spacings of the vortex core levels are not expected to change significantly for magnetic fields small compared to  $H_{c2}$ . Although these features are induced by the  $45^\circ$  grain boundaries, they do not appear to be strongly affected by any disorder associated with the grains. A comparison of the spectra from many similar samples shows that the positions of these induced features are very reproducible from sample to sample and their amplitudes correlate with the strength of the  $45^\circ$  peak in the X-ray  $\phi$  scans.

We suggest that these induced spectral features are due to vortex core excitations. According to T. C. Hsu the dipole transitions between the quasiparticle levels in the vortex core are suppressed when the system is translationally invariant [5,23]. The addition of a symmetric pinning potential breaks the translational symmetry and induces the angular momentum conserving lowest vortex core transition. However, for vortices pinned at a grain boundary the rotational symmetry is also lost allowing, in principle, violation of the angular momentum selection rule and the higher energy transitions [24,25].

For the interpretation in terms of vortex dynamics we consider two scenarios. In the first we take the feature at  $65 \text{ cm}^{-1}$  in  $T^+(H)/T(0)$  as the fundamental of the vortex core resonance. This follows from extensive studies of the magneto-optical properties of Class (1) films which also show this feature [10,19]. Within the Hsu model the vortex core resonance is hybridized with the pinning resonance. The corresponding core level spacing  $\hbar\Omega_0 = E_{1/2} - E_{-1/2}$  is about  $40 \text{ cm}^{-1}$  (where  $\mu = \pm 1/2$  are the angular momentum quantum number of vortex core levels). The higher frequency resonances are then the  $\Delta\mu > 1$  transitions induced by the grain boundaries. In s-wave BCS theory these resonances occur at near multiples of  $\Omega_0$  if  $\hbar\omega \ll 2\Delta$ . In this scenario the resonance at  $80 \text{ cm}^{-1}$  is the second harmonic, corresponding to the transition from  $\mu = -1/2$  to  $\mu = +3/2$  or  $\mu = -3/2$  to  $\mu = +1/2$ . As one can see from the curve fitting described later, this  $80 \text{ cm}^{-1}$  feature appears to be split into a doublet. This splitting may arise from the lifting of the degeneracy of the two transitions due to the grain boundary. The dispersive features at  $116 \text{ cm}^{-1}$  and  $160 \text{ cm}^{-1}$ , occur in both modes with nearly equal strength. We conjecture that these features

are the third and fourth harmonics of the vortex core resonance. However, a splitting such as observed on the second harmonic may also play a role in these transitions, for example, they could be the split third harmonic.

In the second scenario, we regard the  $80 \text{ cm}^{-1}$  feature as the fundamental resonance of the vortex core, the transition from  $\mu = -1/2$  to  $\mu = +1/2$ . According to the dipole selection rules, this resonance should occur in the hCR mode, as observed [24]. In this case the splitting must come from two different types of sites for the vortices on the grain boundaries. Then the features at  $116 \text{ cm}^{-1}$  and  $160 \text{ cm}^{-1}$  are the split second harmonic. However, this interpretation seems to produce a paradox. If the  $65 \text{ cm}^{-1}$  feature in the eCR mode in both Classes of samples is also related to the fundamental of the vortex core resonance, why does the resonance occur at two different frequencies? This problem may be resolved by depolarization shifting of the allowed resonance. Zhu *et al.* [24] have examined the depolarization effect on the response due to the inhomogeneous conductivity of the vortex system. The resonance frequency  $2E_{1/2}$  can be redshifted to  $2(1 - \kappa)E_{1/2}$  in which  $\kappa$  is estimated to be 0.43. This would imply, for the dipole allowed transition, that those vortices in the bulk participate in the response as described by Hsu but are subject to the depolarization effect, while those vortices pinned by  $45^\circ$  grain boundary give rise to a weakly allowed resonance that is not depolarization shifted. A possible difficulty with this interpretation is that the dipole resonance is quenched by the vortex motion, according to Hsu, so that the depolarization shift may, in fact, be small.

The temperature dependence of the magneto-optical spectra from a Class (2) samples is shown in Figure 4. The unpolarized transmission ratio  $T(9T)/T(0)$  is shown for a sample similar to the one used for the low temperature data in Figure 1. In these spectra the resonance at  $80 \text{ cm}^{-1}$  is not as well resolved because the grain boundary induced features in this sample are weaker and they are mixed with the low frequency rise of the pinning resonance. However, we see that the structures at  $110 \text{ cm}^{-1}$  and  $160 \text{ cm}^{-1}$  are present and they are seen to persist up to very high temperatures, remaining discernible at  $55^\circ\text{K}$ . Moreover, the frequency positions of these features do not shift with temperature. This

behavior is very different than predictions for vortex core excitations within the BCS s-wave theory. In this case calculations have shown that when the temperature is comparable with  $E_{1/2}/k_B$  which is about 20°K (40°K) for  $\Omega_0 = 40 \text{ cm}^{-1}$  ( $80 \text{ cm}^{-1}$ ), the  $\mu = 1/2$  level becomes thermally populated with quasiparticles and the self-consistent gap function begins to change its shape. The vortex core broadens and the quasiparticle energy level spacings decrease. The observed behavior would require the gap function in YBCO to be nearly temperature independent as has also been reported from infrared reflectivity measurements [26]. Also, we note that for the case of d-wave superconductors the quasiparticle levels in the vortex core have a number of significant differences from the s-wave case. In addition to the set of localized levels similar to that found in s-wave superconductors there are also continuum levels and additional high energy levels outside the core that are associated with s-wave admixture induced by the vortex [27,28]. Therefore, another possibility is that the high frequency features are related to these levels.

To gain further insight into the nature of these grain boundary induced optical features we have studied their spectral line shapes. We have modeled the conductivity function of the system in terms of Lorentzian oscillators. We start with the analysis of the spectra of the class (1) samples. These spectra can be modeled in terms of Hsu's conductivity function [5,10] or equivalently as two finite frequency oscillators and a zero frequency delta function. To model the class (2) samples we first fit the 12T data in Figure 2 to the Hsu conductivity or its Lorentzian equivalent. The resulting Hsu fitting parameters are  $\omega_c = 3.7 \text{ cm}^{-1}$ ,  $\Omega_0 = 45 \text{ cm}^{-1}$ ,  $\alpha = 48 \text{ cm}^{-1}$ ,  $1/\tau_\alpha = 31 \text{ cm}^{-1}$ . We have then added Lorentzian oscillators to this conductivity function to model the grain boundary induced dispersive features. We have included four new oscillators to model the system

$$\sigma_{total}^\pm = \left(1 - \sum_{i=1}^4 f_i^\pm\right) \sigma_{Hsu}^\pm + \sum_{i=1}^4 f_i^\pm \sigma_i \quad (1)$$

in which

$$\sigma_i = \frac{ne^2}{m} \frac{1}{i(\omega - \omega_i) + 1/\tau_i} \quad (2)$$

where  $f_i^\pm$  represents the strength of the  $i$ th oscillator in two polarization modes. The parameters from the fit are shown in Table I. The results of these fits are shown in Figure 3. We have assumed that there is no contribution in the eCR mode from the first two oscillators near  $80 \text{ cm}^{-1}$  (That is,  $f_1^+ = f_2^+ = 0$ ) because we believe that this resonance is already included in  $\sigma_{Hsu}^+$ . The third and fourth oscillators do not have an obvious chirality and their oscillator strengths are an order of magnitude smaller than the first two. This analysis shows that the dispersive line shapes of the grain boundary induced spectral features in the transmission are consistent with resonances at the center frequencies of these features.

It is interesting to consider the relation of these spectral features to the electronic properties of grain boundaries. Numerous studies have been made of the I-V characteristics of junctions associated with grain boundaries in YBCO films grown on bicrystals [16,17]. Winkler *et al.* [16] reported the observation of Fiske steps at low voltages due to terahertz electromagnetic resonances in grain boundary junctions. These are Josephson effect standing waves in the junction and they are suppressed by a field of a few tenths of gauss. The characteristic field for the suppression,  $\phi_0 / (\lambda_L L)$  (where  $\phi_0$  is the flux quantum,  $\lambda_L$  London penetration depth,  $L$  length of the grain boundary), corresponds to the condition that the junction contains one flux quantum. Chaudhari *et al.* [17] reported periodic structure in the conductance of similar grain boundaries at higher voltages whose field dependence is on a much larger scale. Conductance peaks are found at about 2.4, 4.7, 7.2, and 9.5 mV and they have a very peculiar magnetic field dependence. They find that the conductance peak at 9.5 meV is suppressed when a parallel magnetic field is applied (at about 2T) and is shifted when a perpendicular field is applied. These effects are not understood but the authors suggest that they may be related to quasiparticle levels in the junction. From BCS calculations De Gennes *et al.* [29] predicted quasiparticle levels below the bulk gap in S-N junction that depend on the details of the junction.

However, it does not appear to be possible to relate these effects to our FIR results. This would require that the observed spectral features be present in zero field and become suppressed in applied magnetic fields. However, we do not observe any such features of the

required strength in our zero field transmission spectra as can be seen in the inset of Figure 2. We assume, for example, that there is a zero field structure of 30% which diminishes linearly with field, it would give rise to a 10% change in transmission at 10T (See Fig. 2) and go to zero at  $\simeq 30\text{T}$ . For the Josephson standing waves this would imply a junction of length less than  $10\text{\AA}$  which is unreasonably small. In general it is difficult to obtain a characteristic field of 30T since  $H_{c2} \sim 150\text{T}$ . Also, we note that the reproducibility of the observed spectral features would require a reproducible ordered morphology of the grain boundaries.

From these considerations we believe that these grain boundary related far infrared features are induced by the magnetic field. Therefore it appears that the picture in which these features are vortex core excitations brought about by vortex pinning at  $45^\circ$  grain boundaries is the most plausible interpretation of these magneto-optical experiments. Because the  $80\text{ cm}^{-1}$  feature in the hCR mode has the correct selection rule for the dipole transition, we believe it represents the fundamental  $\Delta\mu = 1$  vortex core resonance. In this case the core spacing, as perturbed by the grain boundary,  $\hbar\Omega_0 \simeq 10\text{meV}$ . A calculation of the depolarization shifted response of vortices in the bulk would help clarify the interpretation.

We acknowledge useful discussions with T. Hsu, C. Kallin, and F.-C. Zhang. This work is partially supported by NFS under Grant No. 9223217.

## REFERENCES

- [1] S. J. Hagen *et al.*, Phys. Rev. **B 47**, 1064 (1993).
- [2] A. T. Dorsey, Phys. Rev. **B 46**, 8376 (1992).
- [3] R. A. Ferrell, Phys. Rev. Lett. **68**, 2524 (1992).
- [4] H. Suhl, Phys. Rev. Lett. **14**, 226 (1965).
- [5] T. C. Hsu, Physica **C 213**, 305 (1993) and Phys. Rev. **B 46**, 3680 (1992).
- [6] N. B. Kopnin, JEPT Lett. **27**, 390 (1978).
- [7] J. R. Clem and M. W. Coffey, Phys. Rev **B 46**, 14662 (1992).
- [8] S. Spielman *et al.*, Phys. Rev. Lett. **73**, 1537 (1994).
- [9] K. Karrai *et al.*, Phys. Rev. Lett. **69**, 355 (1992).
- [10] E.-J. Choi *et al.*, Phys. Rev. **B 49**, 13271 (1994).
- [11] Y. Zhu, Z. L. Wang, and M. Suenaga, Philos. Mag. **A 67**,11 (1993).
- [12] N. D. Browning *et al.*, Physica **C 212**, 185 (1993).
- [13] M. F. Chisholm *et al.*, Interface Science **1**,339 (1993).
- [14] D. Miller *et al.*, Phys. Rev. **B 47**, 8076 (1993).
- [15] S. S. Laderman *et al.*, Phys. Rev. **B 43**, 2922 (1991).
- [16] D. Winkler *et al.*, LT-20 Eugene-93 and Phys. Rev. Lett. **72**,1260 (1994).
- [17] P. Chaudhari *et al.*, Phys. Rev. **B 48**, 1175 (1993).
- [18] S. J. Rosner *et al.*, Appl. Phys. Lett. **60**, 1010 (1992). D. K. Fork *et al.*, J. Mater. Res. **7**, 1641 (1992).
- [19] E.-J. Choi *et al.*,Physica **C**, to be published.

- [20] D. K. Fork *et al.*, Appl. Phys. Lett. **57**, 1161 (1990).
- [21] S. Wu *et al.*, submitted for publication.
- [22] Recently the pinning resonance has been fully resolved in measurements extended down to  $5\text{ cm}^{-1}$  using a FIR laser. Also these measurements reveal the existence of a zero frequency oscillator as has been inferred from microwave studies. These observations are not germane to the subject of this paper and will be published elsewhere.
- [23] H. D. Drew and T. C. Hsu, Phys. Rev. **B**, to be published.
- [24] Y. Zhu, F. Zhang and H. D. Drew, Phys. Rev. **B 47**, 586 (1993).
- [25] B. Janko and J. Shore, Phys. Rev. **B 46**, 9270 (1992).
- [26] R. T. Collins *et al.*, Phys. Rev. **B 43**, 8701 (1991).
- [27] P. I. Soininen, C. Kallin, and A. J. Berlinsky, Phys. Rev. **B 50**, 13883 (1994).
- [28] Y. Ren *et al.*, Phys. Rev. Lett. **74**, 3680 (1995).
- [29] P. G. De Gennes and D. Saint-James, Phys. Lett. **4**, 151 (1963).

## FIGURES

FIG. 1. The transmission ratio  $T^\pm(H)/T(0)$  vs. frequency for YBCO thin films from Class (1) and (2) at 12T and 2.2°K. Class(1): YBCO on Si with only low angle grains. Class (2): YBCO on Si substrate with 45° grains. The circularly polarized response is shown:  $T^+$  for the hCR mode and  $T^-$  for the eCR mode. The region between 125~140  $cm^{-1}$  corresponds to a quartz phonon and the half waveplate condition of the polarizer. The signal to noise ratio deteriorates rapidly below 40  $cm^{-1}$  because of low transmitted spectral intensity.

FIG. 2. The magnetic field dependence of  $T^\pm(H)/T(0)$  of a YBCO thin film of Class (2) at 2.2°K. Fields from top are +12T, +8T, +4T, -4T, -8T, -12T. Several features induced by the 45° grain boundaries become distinct at high fields. There is a dispersive spectral feature centered at 80  $cm^{-1}$  in the hCR mode and features at 116  $cm^{-1}$  and 160  $cm^{-1}$  occur with equal weight in both modes. These features do not shift as field increases and among different Class (2) samples. Inset: Transmission of a class (2) sample at zero field and 4°K. This smooth response corresponds to a simple London-Drude conductivity.

FIG. 3. The results of the line shape analysis of Class (2) magneto-transmission data using Hsu's conductivity plus additional Lorentzian oscillators. The long dashed lines are  $T^\pm(H)/T(0)$  of YBCO thin film from a Class (2) sample in 12T field at 2.2°K. The dotted lines are the fits using only Hsu's vortex dynamics theory. The thick solid lines are the fits including multiple Lorentzian oscillators to model the vortex core excitations. The parameters for the fits are listed in Table I.

FIG. 4. The temperature dependence of the unpolarized transmission ratio  $T(H)/T(0)$  of a YBCO thin film of Class (2) at 9T. The dispersive features at 116  $cm^{-1}$  and 160  $cm^{-1}$  persist to 55°K. Because the grain boundary related features in this sample are weaker the changes of the features at 80  $cm^{-1}$  are not well resolved.

## TABLES

fitting\ith	1st	2nd	3rd	4th
$\omega_i$	$72cm^{-1}$	$90cm^{-1}$	$116cm^{-1}$	$158cm^{-1}$
$\frac{1}{\tau_i}$	$8cm^{-1}$	$16cm^{-1}$	$3.5cm^{-1}$	$8cm^{-1}$
$f_i^+$	0%	0%	0.04%	0.06%
$f_i^-$	0.5%	1.3%	0.06%	0.15%

TABLE I. The parameters of the line shape analysis of the transmission data using the Hsu conductivity and multiple Lorentzian oscillators. The formula for the oscillators is given by Eq.(1) and Eq.(2). See also Fig.3.

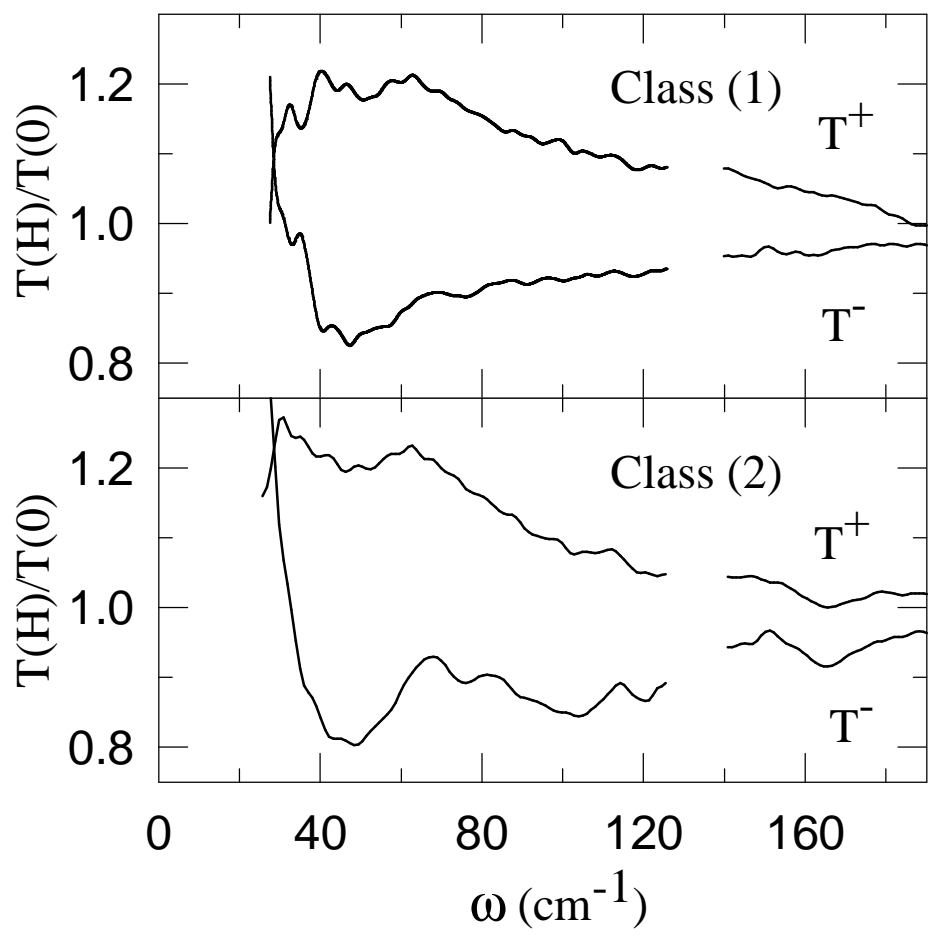


Fig. 1

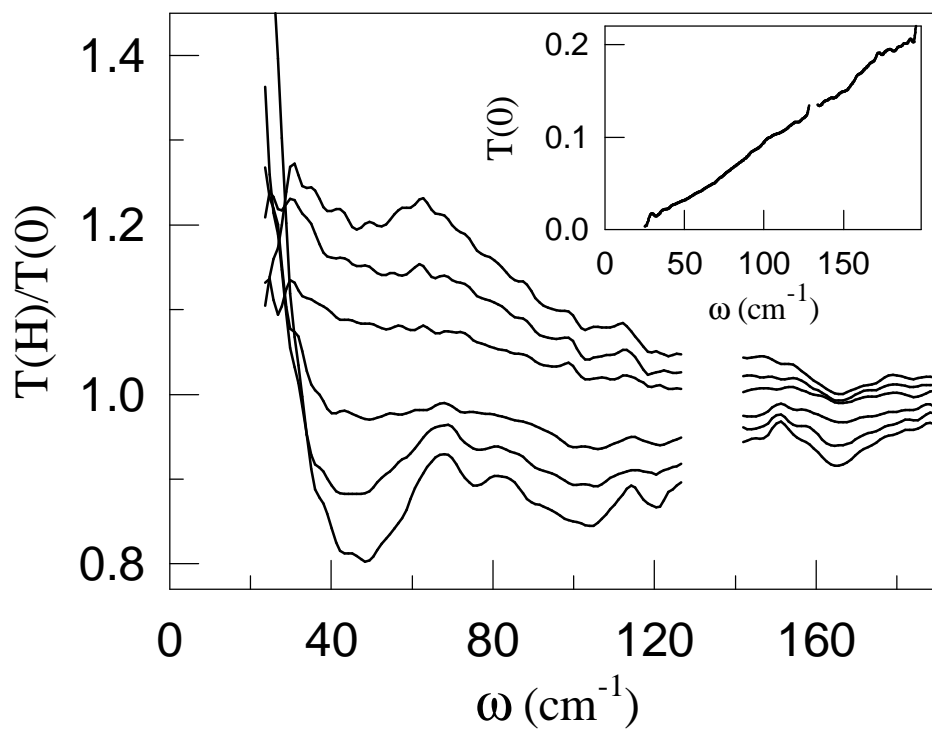


Fig. 2

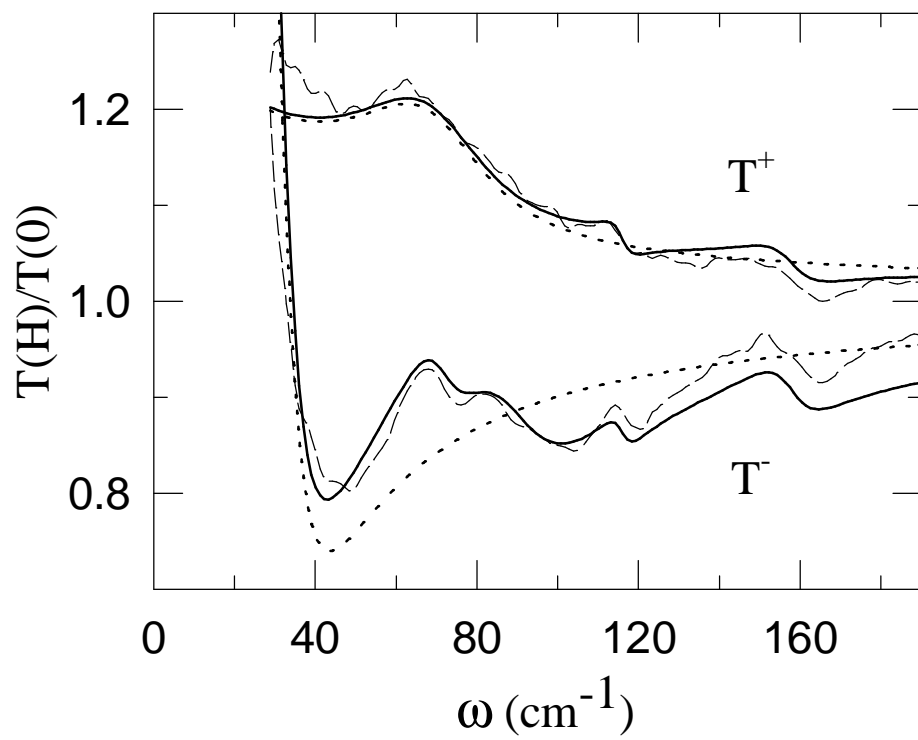


Fig. 3

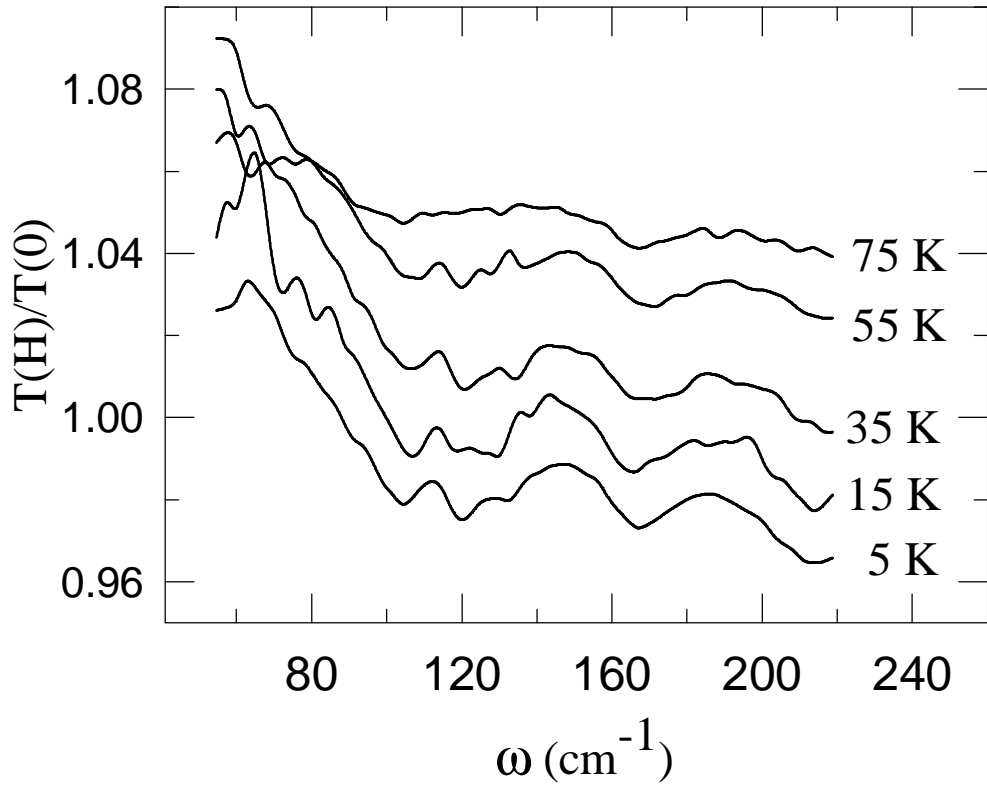


Fig. 4